Indian Journal of Geo Marine Sciences
Vol. 48 (01), January 2019, pp. 25-31

Relationship of LST, NDBI and NDVI using Landsat-8 data in Kandaihimmat Watershed, Hoshangabad, India

Mohammad Subzar Malik[1], Jai Prakash Shukla[2] & Satanand Mishra[*]
Water Resource Management and Rural Technology Group
CSIR-Advanced Materials and Processes Research Institute (AMPRI), Bhopal (M.P) - 462026, India
[*E-mail: snmishra07@gmail.com]

Received 02 August 2017; revised 08 January 2018

Normalized Difference Vegetation Index (NDVI) and Normalized Difference Built-up Index (NDBI) have been computed and their relationships with Land surface temperature (LST) in each season were examined. LST retrieved by thermal data analysis represents the spatial and temporal distribution of surface temperature. NDBI is describing the built-up index and NDVI the proportion of vegetation in the watershed. Relationships of LST with NDBI & NDVI were developed in each season. Correlation results of LST & NDBI has shown strong positive relationship i.e. $R^2 = 0.991$ in Jan.2016, 0.981 in May 2016 & 0.965 in Oct.2016, where as strong negative correlation were found in between LST & NDVI i.e. $R^2 = 0.993$, 0.992, & 0.911 in each season. Relationship between NDVI & NDBI was also developed and is showing strong negative correlation i.e. $R^2 = 0.979$, 0.988, & 0.913.

[**Keywords**: Land surface Temperature; NDBI; NDVI; LANDSAT-8; ArcGIS]

Introduction

Land Surface Temperature (LST) is defined as the temperature at interface between the Earth's surface and its atmosphere[1]. It is an important parameter in all physical processes of surface energy and water balance at local and global scales[2-8]. LST is playing a key role in land surface processes, not only, because of having climatic importance, but also due to its control of the sensible and latent heat flux exchange[9-10]. LST have wide application in many fields viz; evapotranspiration, climate change, hydrological cycle, vegetation monitoring, urban climate and environmental studies[11-18]. LST is also used in models of vegetation stress[19-21] and can be assessed for obtaining climatic trends when observed over many years[22]. Due to the limitations in in-situ observations and relatively large spatial variability in LST, it is commonly measured on a regional or global basis with satellite retrievals. On the availability of large scale satellite obtained LST data, near surface air temperature measurements can be evaluated[23-25]. LST data is useful for monitoring the temperature of different land use land /cover surfaces. It can be often used for checking and predicting of crop yield [26]. Due to the strong heterogeneity of land use/ land cover (LU/LC) surfaces such as vegetation, surface roughness, topography and soil[27-28] LST changes rapidly in space as well as in time [29-30]. Therefore, it requires measurements with detailed spatial and temporal sampling.

Satellite based thermal infrared (TIR) data is directly linked to the LST through the radiative transfer equation. LST retrieval from remotely sensed TIR data has attracted much attention and its history dates back from 1970s[31-32]. Remote sensing technology provides a unique way for evaluating LST on global scale. Remote sensing application is required to observe the spatiotemporal land cover changes in relation to the basic physical properties and in terms of the surface radiance and emissivity data. Remote sensing benefits are having availability of high resolution data, consistent and repetitive coverage and are able to map the earth's surface conditions[33]. Thermal infrared (TIR) sensors are capable of obtaining quantitative information about surface temperature in different land cover classes. There are many workable thermal infrared sensors which are able to study LST viz; Geostationary Operational Environmental Satellite (GOES), NOAA-Advanced Very High Resolution Radiometer (AVHRR), Terra and Aqua- Moderate Resolution Imaging Spectroradiometer (MODIS).High resolution data from the Terra-Advanced Space borne Thermal Emission and Reflection Radiometer (ASTER) has a 90m resolution and LANDSAT-7 Enhanced Thematic Mapper (ETM+) and LANDSAT-8 TIRS having resolution of 100m in thermal region. LST is sensitive to vegetation and soil moisture; therefore, it can be used to observe land use/land cover changes, such as urbanization, desertification etc.

The Spatial and temporal changes resulted in LST due to changes occurred in land us/ land over cover and influence on the local weather of that area. Nowadays urbanization has become a common phenomenon, since the 20th century, about 50% of the population living in the city now[34]. Rapid urbanization leads to an increase in LST, which is governed by surface heat fluxes and play a key role in global climate change. Urbanization results in global climate change in various ways and multiple dimensions. Recent research reported that urban population is expected to reach 65 % by (2025)[35].

Multi-temporal and multi-resolution remote sensing images can provide basic data for analyzing urban spatial information and thermal environment effectively. Previous studies suggest that there exists a strong negative correlation between NDVI and LST, while NDVI changes greatly with season. Normalized difference vegetation index (NDVI) and Enhanced vegetation index (EVI) have been used as an indicator for vegetation cover and Normalized difference built-up index (NDBI) for level of urbanization. NDBI is defined as the linear combination of near infrared band (0.76 ~ 0.90 μm) and the middle infrared (MIR) band (1.55 ~ 1.75 μm), used for extraction of urban built-up land[36]. The present study analyzes the potential of LANDSAT-8 TIRS in mapping of LST and interprets their relationship with NDVI & NDBI using ArcGIS software.

Materials and Methods

Kandaihimmat Watershed form a part of Tawa river basin has been taken under investigation. The watershed covers the total geographical area of 166.58 km^2. The study area falls in survey of India (SOI) Toposheet No. 55 F/14, between latitude (22^0 30' 00"- 22^0 40' 00" N) and longitude (77^0 45' 00"- 78^0 00' 00" E). The watershed contains thick alluvium soil cover with good sources of irrigation facilities and is rich in agriculture. The watershed is part of rural area having wide spread built-up land. The seasonal LST variation was calculated from satellite data in ArcGIS software and inferred their relationship with NDBI and NDVI. Location map of the study area is showing in Fig.1.

Three LANDSAT-8 images acquired on different season's winter 23 January 2016, summer 30 May 2016 & rainy 21 Oct, 2016 were downloaded from

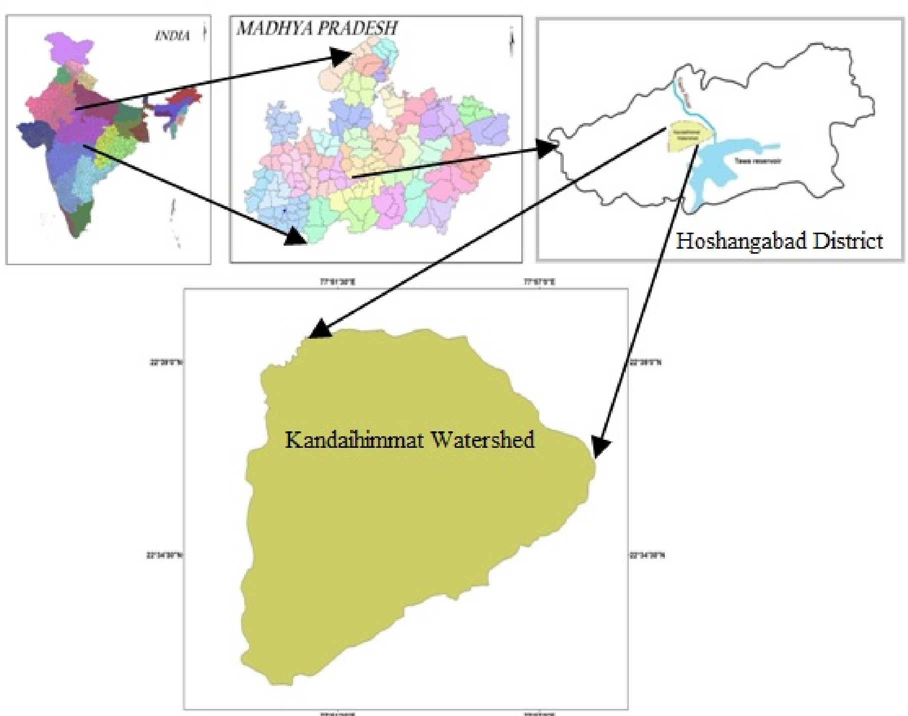

Fig. 1 — Location Map of the study area

USGS earth explorer web, has been used in the study. Satellite data analysis was done in ArcGIS software. Band 6 and Band 5 of the satellite imagery were processed for extracting the built-up index, while Band 4 & Band 5 of the data was processed for NDVI analysis. Thermal band TIRS (Band 10) was analyzed for surface temperature retrieval. In the proceeding paragraphs we have explained the complete processes of extracting these features from the satellite data by using ArcGIS software.

NDBI stands for Normalized Difference Built-up Index, In comparison to the other land use / land cover surfaces, built-up lands have higher reflectance in MIR wavelength range (1.55~ 1.75µm) than in NIR wavelength range (0.76~ 0.90µm). NDBI is very useful for mapping the urban built-up areas and has been computed using the equation (1) expressed as follows;

$$NDBI = \frac{MIR\ (band\ 6) - NIR\ (Band5)}{MIR\ (band\ 6) + NIR\ (band5)} \quad \text{... (1)}$$

Where, MIR is middle infrared reflectance, which is band 6 of Landsat-8. NIR is near infrared reflectance such as band 5 of Landsat-8; NDBI values range from -1 to 1. The greater the NDBI is, the higher the proportion of built-up area is.

Normalized Difference Vegetation Index (NDVI) is an index that describes the vegetation proportion by measuring the difference in the near-infrared portion of electromagnetic spectrum which is strongly reflected by green vegetation and red portion of the spectrum which is absorbed by vegetation. NDVI were calculated by using NIR Band 5 and Red Band 4 of the Landsat-8 data by given below equation (2) in ArcGIS software. The calculation of the NDVI is important because, the proportion of the vegetation (P_V) will be calculated and they are highly related with the NDVI and emissivity (ε) is calculated, which is related to the P_V:

$$NDVI = \frac{NIR(band5) - R(band4)}{NIR\ (band5) + R(band4)} \quad \text{… (2)}$$

Where, NIR represents the near-infrared band (Band 5) and R represents the red band (Band 4)

Land surface temperature is the temperature at the interface of earth's surface with its atmosphere. It can be measured from the ground surface up to the height of 2-3m. While calculating of LST from the Landsat-8 satellite data, different mathematical algorithms were used and processed in ArcGIS software. Evaluation of LST, from LANDSAT-8 data in ArcGIS raster processing involving the following steps:

1. Conversion of satellite digital number into radiance by:

$$\mathrm{L\lambda = ML * Qcal\ + AL - Oi} \quad \text{… (3)}$$

Where, ML represents the band-specific multiplicative rescaling factor, Qcal is the Band 10 image, AL is the band- specific additive rescaling factor, and Oi is the correction for Band 10.

2 Conversion of Radiance to At-Sensor Temperature by;

$$\mathrm{BT} = \mathrm{K2}\ /\ln\ [(K1/L\lambda) + 1] - 273.15. \quad \text{… (4)}$$

Where, Tb is effective at satellite temperature in absolute temperature, K_1 and K_2 stand for the band-specific thermal conversion constants from the metadata. For obtaining the results in Celsius, the radiant temperature is revised by adding the absolute zero ($-273.15\ ^0$C)

3. Conversion of Satellite Brightness Temperature into LST by;

$$Ts = \mathrm{BT}/\ \{1 + \lambda\ (\mathrm{BT}/\rho)\ \ln \varepsilon\lambda]\} \quad \text{… (5)}$$

Where Ts is the LST in Celsius (^{0}C), BT is at-sensor BT (^{0}C), λ is the wavelength of emitted radiance (λ = 11.5 µm) $\varepsilon\lambda$ is the emissivity.

While in conversion of satellite brightness temperature in to land surface temperature we have required of emissivity which have been calculated from NDVI by using the below given formula in ArcGIS.

$$\mathrm{e = 0.004Pv + 0.986} \quad \text{… (6)}$$

Where e is the emissivity calculated from the proportion of vegetation (Pv) by using following formula:

$$Pv = \frac{[NDVI - NDVIs\ ]^2}{[NDVIv + NDVIs]} \quad \text{… (7)}$$

Where, the $\mathrm{NDVI_s}$ and $\mathrm{NDVI_v}$ are the thresholds of soil and vegetation pixel.

Results and Discussion

Land surface temperature acquired from satellite data represents the surface temperatures of each object within a pixel, which may be composed of several land cover types. With the help of above described equations processing of Landsat-8 thermal band 10, has been done in ArcGIS and LST maps of the study area were prepared. LST maps (Fig. 2a-c)

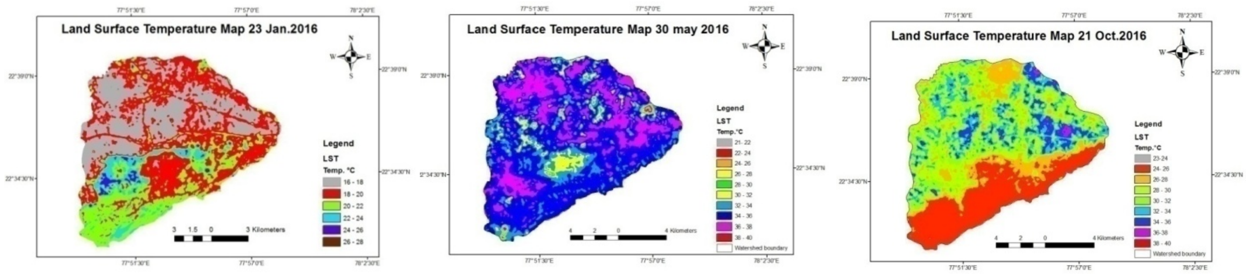

(a) (b) (c)

Fig. 2(a— c)-Land Surface Temperature Maps

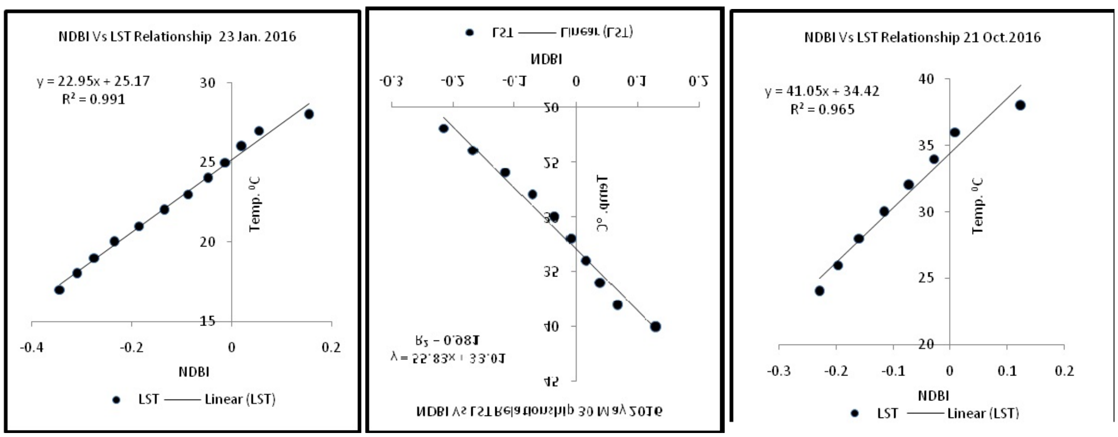

a b c

Fig. 3 (a-c) — NDBI Vs LST Relationship

Table 1 — Statistics of Land Surface Temperature

Date	Minimum LST (^{0}C)	Maximum LST (^{0}C)
23 Jan. 2016	18	28
30 May 2016	22	40
21 Oct.2016	24	38

were prepared are showing the spatial distribution of surface temperature within the watershed. The different thermal signatures seen in the LST maps of the watershed are because of the different land cover classes having different physical properties. The statistics showing minimum & maximum values of LST is given in Table 1.

Land Surface Emissivity

Land surface emissivity is a proportionality factor that scales black-body radiance to predict emitted radiance. It led significant impact on LST. Schadlich et al., 2001 & Sobrino et al. 2004[37-38] have made an assumption that land cover is soil when the NDVI value is below 0.2 and vegetation when it is over 0.5. Emissivity have been derived from Landsat-8 satellite data by calculated the proportion of vegetation with the help of algorithm 6 & 7 in ArcGIS software. The maximum & minimum values of emissivity derived are given in Table 2.

Table 2 — Emissivity values derived from Landsat-8 data

Date	Minimum	Maximum
23 Jan. 2016	0.9863	0.9874
30 May 2016	0.9860	0.9876
21 Oct.2016	0.9860	0.9878

NDBI and LST Relationship

During the study relationship between NDBI and LST were developed and found direct relationship between them in each season. Results of NDBI have shown the maximum surface temperature in Built-Up areas. Therefore, it have been predicted that built-up areas or urbanization is a inducing much surface temperature variations. In NDBI & LST correlation a strong positive relationship has been existed in each season i.e. R^2 = 0.991, 0.981 & 0.965 in Jan. May & Oct. 2016 (Fig. 3a-c).The positive relationship found between NDBI and LST indicates that built-up area is generating much surface temperature variations and is the key contributor in urban heat island. On the other hand, healthy vegetative cover plays a key role in lowering of the surface temperature. Statistical detail of NDBI is given in Table 3.

NDVI and LST Relationship

Normalized Difference Vegetation Index (NDVI) is a measure of the amount and vigor of vegetation at the surface[39]. NDVI is very sensitive to changes and variations of NDVI might cause changes in land surface temperature. NDVI and LST relationship changed with season to season, but without obvious regularity. Correlation analysis has been done to find out the relationship between LST and NDVI which have shown a strong negative correlation i.e. R^2 = 0.993 in winter (Jan.2016) 0.992 in summer (May 2016) and 0.971 in rainy season (Oct.2016) (Fig. 4a-c). From our observations, high surface temperature was observed in built-up and bare surfaces where as low surface temperature in green vegetative areas. Statistics of NDVI is given in Table 4.

NDVI and NBDI Relationship

Relationship between NDVI and NBDI has also been developed during the study. The minimum and maximum range of NDBI in each seasons varies from - 0.3048, 0.1536, -0.2156, 0.1285 and -0.2296, 0.1246 respectively. NDVI have shown strong negative relationship with NDBI in each season i.e. R^2 = 0.979 in Jan. 0.988 May & 0.913 in Oct. NDVI can be used to characterize the evolution and expansion of built-up land[40]. The linear correlation of NDVI Vs NDBI is displaying in the scatter plot (Fig. 5a-c).

Table 3 — Statistics of NDBI

Date	Minimum	Maximum	Mean
23 Jan. 2016	-0.3048	0.1536	-0.0977
30 May 2016	-0.2156	0.1285	-0.0360
21 Oct.2016	-0.2296	0.1246	-0.0834

Table 4 — Statistics of NDVI

Date	Minimum	Maximum	Mean
23 Jan. 2016	-0.3048	0.1536	-0.0977
30 May 2016	-0.2156	0.1285	-0.0360
21 Oct.2016	-0.2296	0.1246	-0.0834

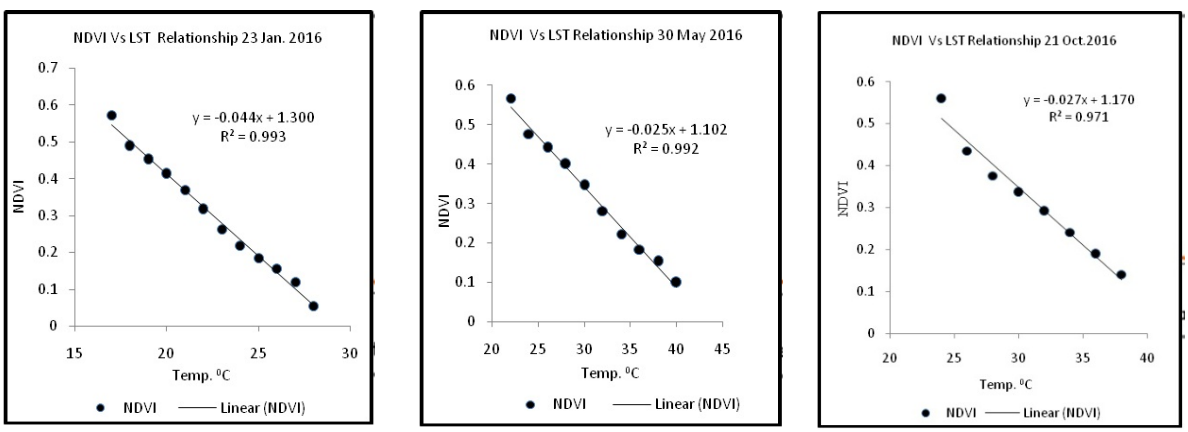

a b c

Fig. 4(a-c) — NDVI Vs LST Relationship

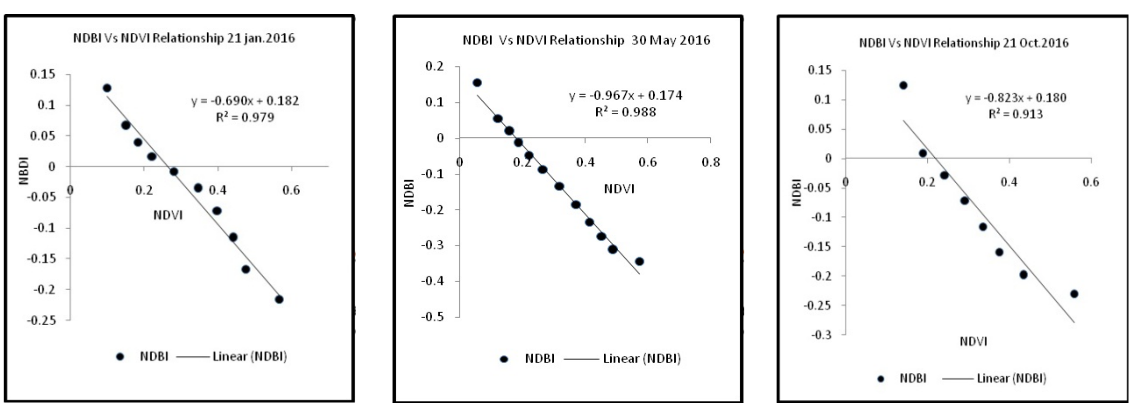

a b c

Fig. 5(a-c) — NDBI Vs NDVI Relationship

Conclusion

LST maps were prepared from satellite data analysis represents the spatial distribution of surface temperature in the watershed.LST analysis has shown higher surface temperature in built-up and bare surfaces and low in healthy vegetated areas. The maximum LST observed in each season was 28, 40 and 38^{0}C respectively. NDBI evaluated from Band 6 & Band 5 of the satellite data is describing the built-up index. The maximum NDBI in each season was 0.1536, 0.1285 & 0.1246 respectively. In summer NDBI and LST found significantly correlated i.e. (R^2=0.981). Emissivity's estimates were also retrieved using the classification-based algorithm in ArcGIS. Emissivity has shown inverse relationship with LST. The developed correlation of LST with NDBI and NDVI has shown R^2 = 0.991 & 0.993 in jan.2016, 0.981 & 0.992 in May 2016, 0.965 & 0.911 & in Oct.2016. Strong negative correlation resulted between NDVI & NDBI i.e. R^2 = 0.979, 0.988 & 0.913 for jan.2016, May 2016 & Oct.2016 respectively. The strong positive correlation found between LST and NDBI means more be the built-up area high is the surface temperature. The strong negative correlation of NDVI with LST indicates that healthy green vegetation lowers the surface temperature. Thus, it can be suggested that NDBI not only can be used to analyze and predict LST but also can be used to draw the urban heat island effect in any area and provides a reliable basis for urban construction and planning.

Acknowledgement

Authors are thankful to *Director, CSIR-AMPRI, Bhopal,* for giving permission to publish this Research Article. We also acknowledge the financial support provided by *MPCST*, *Bhopal*, during the study.

References

1 Niclòs, R., Valiente, J.A., Barberà, M.J., Estrela, M.J., Galve, J.M. & Caselles, V., Preliminary results on the retrieval of land surface temperature from MSG-SEVIRI data in Eastern Spain, in *EUMETSAT 2009: Proceedings of Meteorological Satellite Conference* (2009) 21-25.

2 Brunsell, N.A., & Gillies, R.R, Length scale analysis of surface energy fluxes derived from remote sensing. *Journal of Hydrometeorology*, (2003)4 1212–1219.

3 Rodell, M., & Coauthors, The global land data assimilation system. *Bull. Amer. Meteor. Soc.,* (2004) 85 381–394.

4 Jiang, G.M., Li, Z.L. & Nerry, F., Land surface emissivity retrieval from combined mid-infrared and thermal infrared data of MSG-SEVIRI. *Remote Sensing of Environment,* (2006)105 326–340.

5 Anderson, M. C., Norman, J. M., Kustas, W. P., Houborg, R., Starks, P. J., & Agam, N., A thermal-based remote sensing technique for routine mapping of land-surface carbon, water and energy fluxes from field to regional scales. *Remote Sensing of Environment,* (2008), 112, 4227–4241.

6 Zhang, R., Tian, J., Su, H., Sun, X., Chen, S., & Xia, J., Two improvements of an operational two-layer model for terrestrial surface heat flux retrieval. *Sensors,* (2008), 8, 6165–6187

7 Kustas, W., & Anderson, M. Advances in thermal infrared remote sensing for land surface modeling, *Agricultural and Forest Meteorology*, (2009), 149, 2071–2081.

8 Karnieli, A., Agam, N., Pinker, R. T., Anderson, M., Imhoff, M. L., & Gutman, G. G. Use of NDVI and land surface temperature for drought assessment: Merits and limitations. *Journal of Climate*, (2010), 23, 618–633

9 Aires, F., Prigent, C., Rossow, W. B., & Rothstein, M. A new neural network approach including first guess for retrieval of atmospheric water vapor, cloud liquid water path, surface temperature, and emissivities over land from satellite microwave observations. *Journal of Geophysical Research*, (2001), 106 (D14) 14887–14907.

10 Sun, D., & Pinker, R.T., Estimation of land surface temperature from a Geostationary Operational Environmental Satellite (GOES-8). *Journal of Geophysical Research,* (2003)108, 43-26.

11 Bastiaanssen, W. G. M., Menenti, M., Feddes, R. A., & Holtslag, A.A.M., A remote sensing surface energy balance algorithm for land (SEBAL) Formulation. *Journal of Hydrology*, (1998) 212 198–212

12 Kogan, F. N., Operational space technology for global vegetation assessment, *Bulletin of the American Meteorological Society*, (2001)82 1949–1964.

13 Su, Z., The Surface Energy Balance System (SEBS) for estimation of turbulent heat fluxes. *Hydrology and Earth System Sciences,* (2002)6 85–100.

14 Arnfield, A. J., Two decades of urban climate research: a review of turbulence, exchanges of energy and water, and the urban heat island. *International Journal of Climatology*, (2003) 23 1–26.

15 Voogt, J. A., & Oke, T. R., Thermal remote sensing of urban climates, *Remote Sensing of Environment,* (2003) 86, 370–384.

16 Weng, Q., Lu, D., & Schubring, J., Estimation of land surface temperature vegetation abundance relationship for urban heat island studies, *Remote Sensing of Environment,* (2004)89, 467–483.

17 Kalma, J. D.,McVicar, T. R., &McCabe,M. F., Estimating land surface evaporation: A review of methods using remotely sensed surface temperature data. *Surveys in Geophysics,* (2008) 29, 421–469

18 Weng, Q., Thermal infrared remote sensing for urban climate and environmental studies: methods, applications, and trends. *ISPRS Journal of Photogrammetry and Remote Sensing*, (2009)64, 335–344.

19 Jackson, R. D., S. B. Idso, R. J. Reginato, and P. J. Pinter Jr., Canopy temperature as a crop water stress indicator, *Water Resour. Res.,* (1981) 17, 1133–1138

20 Moran, M. S., Clarke, T. R., Inoue, Y., &. Vidal, A., Estimating crop water deficit using the relation between surface air temperature and spectral vegetation index. *Remote Sens. Environ.,* (1994)49, 246–263

21 Anderson, M. C., Norman, J. M., Mecikalski, J. R., Otkin, J.A., & Kustas, W.P., A climatological study of evapotranspiration and moisture stress across the continental United States based on thermal remote sensing: Surface moisture climatology. *J. Geophys. Res.,* (2007) 112(D10).

22 Jin, M., Analysis of land skin temperature using AVHRR observations, *Bull. Amer. Meteor. Soc.,* (2004)85, 587–600.

23 Cresswell, M. P., Morse, A.P., Thomson, M.C., & Connor, S.J., Estimating surface air temperatures, from Meteosat land surface temperatures, using an empirical solar zenith angle. *Int. J. Remote Sens.,* (1999)20, 1125–1132.

24 Prihodko, L., & Goward, S.N., Estimation of air temperature from remotely sensed surface observations. *Remote Sens. Environ*., (1997) 60, 335–346

25 Stisen, S., I. Sandholt, A., Norgaard, R., Fensholt., & Eklundh, L., Estimation of diurnal air temperature using MSG SEVIRI data in West Africa. *Remote Sens. Environ,* (2007)110, 262–274.

26 Rafiq, M., Rashid, I., & Romshoo, S. A., Estimation and validation of Remotely Sensed Land Surface Temperature in Kashmir Valley, *Journal of Himalayan Ecology & Sustainable Development*, (2014)9

27 Liu, Y., Hiyama, T., & Yamaguchi, Y., Scaling of land surface temperature using satellite data, A case examination on ASTER and MODIS products over a heterogeneous terrain area, *Remote Sensing of Environment*, (2006)105, 115–128.

28 Neteler, M., Estimating daily land surface temperatures in mountainous environments by reconstructed MODIS LST Data, *Remote Sensing*, (2010)2, 333–351.

29 Vauclin, M., Vieira, R., Bernard, R., & Hatfield, J. L., Spatial variability of surface temperature along two transects of a bare, *Water Resources Research*, (1982)18, 1677–1686.

30 Prata, A. J., Caselles, V., Coll, C., Sobrino, J. A., & Ottlé, C., Thermal remote sensing of land surface temperature from satellites: Current status and future prospects, *Remote Sensing Reviews*, (1995), 12, 175–224.

31 McMillin, L.M., Estimation of sea surface temperature from two infrared window measurements with different absorptions, *Journal of Geophysical Research*, (1975) 80, 5113–5117.

32 Carlson, T.N. Augustine, J.A., & Boland, F. E., Potential application of satellite temperature measurements in the analysis of land use over urban areas, *Bulletin of the American Meteorological Society,* (1977)58,1301–1303.

33 Owen, T.W., Carlson, T.N. & Gillies, R.R., Remotely sensed surface parameters governing urban climate change, *Internal Journal of Remote Sensing*, (1998)19, 1663- 1681.

34 United Nations, *"World Urbanization Prospects*: *The 2005 Revision, Database, New York*: Department of Economic and Social Affairs, Population Division," 2006

35 UNFPA *The state of world population 2007: Unleashing the potential of urban growth.* United Nations Population Fund, (United Nations Publications)

36 Zha, Y., An Effective Approach to Automatically Extract Urban Landuse from TM Imagery, *Journal of Remote Sensing*, (2003)1, 37–41,

37 Schadlich, S., Göttsche, F., Olesen, F.S., Influence of land surface parameters and atmosphere on METEOSAT brightness temperatures and generation of land surface temperature maps by temporally and spatially interpolating atmospheric correction, *Remote Sens Environ,* (2001)75(1) 39–46

38 Sobrino, J.A., Jiménez-Muñoz, J.C., Paolini, L., Land surface temperature retrieval from LANDSAT TM 5, *Remote Sens Environ,* (2004) 90(4) 434–440

39 Sundara Kumar, K., Udaya Bhaskar, P., Padmakumari, K., Estimation of Land Surface Temperature to Study Urban Heat Island Effect Using Landsat Etm+ Image, *International Journal of Engineering Science and Technology* (2012) 4 (02)

40 Chen, L., Li, M., Huang, F., & Xu, S., Relationships of LST to NDBI and NDVI in Wuhan City based on LANDSAT ETM+ Image, *in 6th International Congress on Image and Signal, Processing* (CISP2013).